



ARTICLE OPEN



Characterizing immune perturbations in peripheral blood following the East Palestine, Ohio train derailment

Sheridan B. Wagner¹, Hami Hemati¹, Siva Gandhapudi¹, Timothy J. Hilbert², Candace Brancato³, Erin N. Haynes^{2,4}✉ and Ilhem Messaoudi¹  

© The Author(s) 2026

BACKGROUND: The East Palestine, Ohio, train derailment on February 3rd, 2023, resulted in the exposure of residents and the surrounding area to numerous hazardous chemicals, which included known acute irritants and human carcinogens. Despite evacuation and cleanup, both residents and responders reported high occurrences of symptoms associated with exposure in the months following, such as eye, skin, and respiratory irritation, headaches, and fatigue. The long-term health consequences for residents remain uncertain.

OBJECTIVE: To assess the potential for immune perturbations resulting from the exposure, we performed a broad investigation of circulating immune cells and mediators from residents of East Palestine, OH, 5 months following the derailment.

METHODS: We performed exploratory immunophenotyping via flow cytometry and immune mediator profiling via Luminex on peripheral blood mononuclear cells and plasma collected from 19 participants who resided within an approximately one-mile radius of the derailment. These results were compared to sex and age-matched controls from an unexposed location.

RESULTS: Immunophenotyping of East Palestine residents revealed decreased overall proportions of T and B lymphocytes and a shift towards memory subsets. Natural killer cell percentages were increased, particularly the cytotoxic CD56dim subset. Cytokine assays demonstrated heightened levels of cytokines and growth factors associated with hematopoietic differentiation and tissue repair.

SIGNIFICANCE: Collectively, our observations demonstrate potential immunomodulation indicative of a response to an inflammatory insult within this cohort of exposed participants. This investigation indicates the necessity of expanded retrospective studies to continue immune monitoring of residents for evaluation of long-term health impacts.

IMPACT: This study evaluates immune perturbations in East Palestine, OH, residents five months after the February 3rd, 2023, train derailment, revealing altered lymphocyte frequencies, increased cytotoxic NK cells, and elevated cytokines linked to regulation of hematopoiesis and tissue repair. Findings suggest persistent immunomodulation consistent with prior inflammatory exposure and underscore the need for expanded long-term immune monitoring to understand potential chronic health effects in this exposed community.

Keywords: Volatile organic compounds; Disease; Dioxins; Vinyl chloride; inflammation

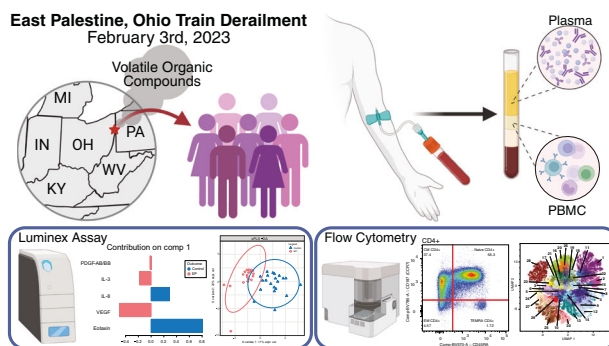
Journal of Exposure Science & Environmental Epidemiology; <https://doi.org/10.1038/s41370-026-00918-y>

¹Department of Microbiology, Immunology, and Molecular Genetics, College of Medicine, University of Kentucky, Lexington, KY, USA. ²Center for the Environment, University of Kentucky, Lexington, KY, USA. ³Department of Biostatistics, College of Public Health, University of Kentucky, Lexington, KY, USA. ⁴Department of Epidemiology and Environmental Health, College of Public Health, University of Kentucky, Lexington, KY, USA. ✉email: erin.haynes@uky.edu; ilhem.messaoudi@uky.edu

Received: 11 December 2025 Revised: 24 April 2026 Accepted: 30 April 2026

Published online: 15 May 2026

Graphical Abstract



INTRODUCTION

On February 3rd, 2023, a freight train transporting hazardous chemical materials derailed in East Palestine, Ohio. Twenty of the derailed freight cars contained hazardous materials, which included known respiratory irritants and human carcinogens [1] (vinyl chloride [2], butyl acrylate [3], ethylhexyl acrylate [4], isobutylene [5], ethylene glycol monobutyl ether [6], and benzene residue [7]). These chemicals were subsequently released into the environment as cars caught fire and their contents drained into nearby water streams [1]. The derailment prompted an evacuation of nearby residents, with officials warning of a potential explosion [8]. To avert this, the five cars containing vinyl chloride underwent a “vent and burn” on February 6th, releasing toxic fumes into the atmosphere [9]. Officials declared on February 8th that it was safe for residents to return, citing that air contaminant levels were below safety screening thresholds [10]. However, a health survey conducted within a month of the derailment indicated high occurrences of headaches (74%), anxiety (64%), coughing (61%), tiredness/fatigue (58%), and irritation, pain, or burning of the skin (52%) [11]. Acute symptoms of irritant exposure among residents and responders were noted in surveys during the months after the derailment [12].

Concerns have been raised over the sensitivity of deployed screening methods to detect low but harmful concentrations and the lack of monitoring for potential chemical derivatives that resulted from the event [13, 14]. Air monitoring studies during the month following the accident revealed high concentrations of acrolein (a combustion product and known respiratory irritant) and identified elevated levels of unique chemical compounds that were not included in regular monitoring [13]. The long-term health consequences of the event on residents remain uncertain. The potential for vinyl chloride exposure is of particular concern due to its association with increased risk of several cancers and cardiovascular disease [15–18]. Such concerns warrant the continued health monitoring of those exposed to the East Palestine (EP) derailment to determine any long-term health impact.

Despite measured levels of released compounds being reported as below minimal risk thresholds, the symptoms reported by East Palestine residents and first responders align with those of volatile organic compound (VOC) exposure [19]. Exposure to environmental pollutants is known to contribute to immune dysregulation, with vinyl chloride and butyl acrylate being linked to the induction of inflammation and disruption of cytokine production [20–22]. Thus, we performed exploratory immune phenotyping and cytokine profiling to assess potential impacts on resident immune regulation using blood samples obtained from 19 participants who resided within an approximately one-mile radius from the derailment.

MATERIALS AND METHODS

Human participants

Whole blood samples were collected on July 17–18th, 2023, from 19 residents of East Palestine, OH, approximately 5 months following the train derailment of February 3rd, 2023. EP participants all resided between 0.3 and 1.6 miles from

the derailment, and all but one evacuated by February 6th. The majority (72.3%) of participants returned between February 8th and 13th. One returned on February 26th. Three individuals did not return as of July 17th, 2023. For controls, we utilized samples from 21 healthy individuals (age and sex matched) who resided in Riverside (California) and were obtained between March 2015 and July 2016 for an unrelated study evaluating varicella zoster virus immunity among a generally healthy population (Table 1). Sex distribution did not differ significantly between East Palestine participants and controls (p -value: >0.9999 , Fisher’s exact test). Differences in age between the two groups, regardless of sex, were also non-significant (p -value: 0.8367, unpaired t -test with Welch’s correction). When analyzed separately by sex, the age difference remained non-significant for both male (p -value: 0.1483) and female participants (p -value: 0.1652). Enrolled participants in both cohorts self-reported as non-smokers. Both studies were approved by the Institutional Review Board at the University of Kentucky (IRB#86158) and the University of California, Riverside (IRB# HS 14-089).

Sample collection and processing

Whole blood samples were collected in EDTA vacutainers. Complete blood counts were obtained with a Cell-DYN Emerald Hematology Analyzer (Abbott, Abbott Park, IL). Samples were processed as previously described [23, 24]. In short, plasma was obtained from maternal whole blood samples with SepMate PBMC Isolation Tubes (STEMCELL, Vancouver, Canada) and Lymphoprep (STEMCELL, Vancouver, Canada) per the manufacturer’s instructions. The buffy coat was removed and centrifuged at 2000 rpm for 5 min before peripheral blood mononuclear cells were resuspended in 10% DMSO and FBS freezing media. Cells were stored in liquid nitrogen, and plasma samples were stored at -80°C .

Luminex

Cytokine, chemokine, and growth factor immune mediator measurements in plasma samples were determined with a Milliplex Human Cytokine/Chemokine/Growth Factor Panel A 38 Plex Premixed Magnetic Bead Panel (MilliporeSigma, Burlington, MA). Plates were analyzed using a MAGPIX instrument and xPONENT software (Luminex, Austin, TX).

Flow cytometry analysis of PBMC

5×10^5 freshly thawed PBMCs were stained with ghost dye UV450 (Tonbo, San Diego, CA) followed by a surface cocktail of the following fluorescently labeled antibodies—CD56 (BUV615; BD Biosciences, Franklin Lakes, NJ), CD3 (BV650; BD Biosciences, Franklin Lakes, NJ), CD14 (BV711; BD Biosciences, Franklin Lakes, NJ), CD8 (cFluor B548; Cytek Biosciences, Fremont, CA), CD4 (cFluor V610; Cytek Biosciences, Fremont, CA), CD20 (PerCP-Cy5.5; BioLegend, San Diego, CA), HLA-DR (APC-Cy7; BioLegend, San Diego, CA), CD11c (BUV661; BD Biosciences, Franklin Lakes, NJ), CD45RA (BV570; BioLegend, San Diego, CA), CD27 (cFluor YG584; Cytek Biosciences, Fremont, CA), IgD (BV605; BioLegend, San Diego, CA), CD123 (PE-CF594; BD Biosciences, Franklin Lakes, NJ), CD16 (BUV395; BD Biosciences, Franklin Lakes, NJ), and CD197 (BV785; BioLegend, San Diego, CA). After a 30-minute incubation, cells were fixed for 2 h, then permeabilized using the Foxp3/Transcription Factor Staining Buffer Kit (Tonbo, San Diego, CA) and stained intranuclearly with Ki67 overnight (BV421; BD Biosciences, Franklin Lakes, NJ). Sample measurements were acquired on an Aurora cytometer (Cytek, Fremont, CA) and analyzed using the SpectroFlo Software (Cytek, Fremont, CA). The cells were unmixing with the autofluorescence extraction option enabled, and extracted FCS files were analyzed using FlowJo (Ashland, Oregon). Manual gating was performed as shown in

Table 1. Cohort metadata.

	East Palestine			Controls		
	Total	Male	Female	Total	Male	Female
Age, n	19	8	11	21	9	12
Mean (SD)	55 ± 15	63 ± 12	49 ± 14	56 ± 15	53 ± 15	58 ± 14
Range	31–76	38–76	31–67	31–77	36–77	31–69
Age Group, n (%)						
20–29 years	5 (26.3%)	1 (12.5%)	4 (36.36%)	5 (23.8%)	1 (11.1%)	4 (33.3%)
40–59 years	5 (26.3%)	1 (12.5%)	4 (36.36%)	6 (28.6%)	1 (11.1%)	5 (41.7%)
60 years	9 (47.4%)	6 (75.0%)	3 (27.27%)	10 (47.6%)	7 (77.8%)	3 (25.0%)

Supplementary Fig. 1B. Unsupervised clustering and dimensionality reduction were performed using FlowSOM (Flow cytometry data analysis using Self-Organizing Maps) [25]. Debris, doublets, and dead cells were excluded from analysis. Outliers with heightened MFI values in one or more clusters were confirmed with the ROUT ($Q = 1\%$) test and excluded from FlowSOM analysis, leaving $n = 17$ in both groups. We down-sampled 29,411 events per sample, concatenated, and exported an FCS file of 999,974 events. The batch effect was corrected with cyCombine (Cofactor: 6000; SOM Grid Size: 8×8; Z-score normalization). Unsupervised clustering and metaclustering were performed using FlowSOM (Metacluster #: 30; SOM Grid Size: 10×10) based on the expression of 15 markers—HLA-DR, CD16, CD56, CD11c, Ki-67, CD45RA, IgD, CD3, CD14, CD197, CD20, CD8, CD4, CD27, and CD123. Dimensionality reduction by UMAP was performed to visualize the data.

Bacterial stimulation

5×10^5 PBMCs were cultured for 16 h in RPMI media with 10% FBS in the presence or absence of a cocktail of bacterial toll-like receptor ligands consisting of 1 µg/mL Pam3CSK4, 0.5 µg/mL FSL-1, and 0.5 µg/mL LPS (Invivogen; San Diego, CA) in 96-well tissue culture plates at 37 °C in a 5% CO₂ incubator. Cells were then stained with the following fluorescently labeled antibodies—CD3 (BV510; BioLegend, San Diego, CA), CD20 (BV510; BioLegend, San Diego, CA), HLA-DR (APC-Cy7; BioLegend, San Diego, CA), CD14 (PE; Invitrogen, Waltham, MA), CD56 (BV711; BioLegend, San Diego, CA), CD16 (AF700; BioLegend, San Diego, CA), CD11c (PE-Cy7; BioLegend, San Diego, CA), and CD123 (BV605; BioLegend, San Diego, CA). Cells were fixed and permeabilized using Biolegend Fixation and Intracellular Staining Permeabilization Wash Buffer (San Diego, CA) before the addition of the following intracellular antibodies—TNFα (APC; BioLegend, San Diego, CA), IL-6 (FITC; Invitrogen, Waltham, MA), IL-1β (PB; BioLegend, San Diego, CA), and MIP-1β (PerCP-eFluor710; Invitrogen, Waltham, MA). Samples were acquired with the Attune NxT Flow Cytometer (Invitrogen, Waltham, MA) and analyzed using FlowJo software (Ashland, OR).

Statistical analysis

Data were analyzed with Prism 10 (GraphPad, Boston, MA). Differences in sex between East Palestine and control participants were determined via Fisher's exact test. Data sets were tested for normality using the Shapiro-Wilk test. Normally distributed data sets were analyzed using an unpaired t-test with Welch's correction. Data sets that were not normally distributed were analyzed using a nonparametric Mann-Whitney test. A sparse Partial Least Squares Discriminant Analysis (sPLS-DA) of plasma immune mediator concentrations was performed for EP and control using the package MixOmics [26].

Ethical approval

The studies to obtain East Palestine and control samples were approved by the Institutional Review Board at the University of Kentucky (IRB#86158) and the University of California, Riverside (IRB# HS 14-089), respectively. Informed consent was obtained from all subjects. All methods were performed in accordance with the relevant guidelines and regulations.

RESULTS

Altered innate and adaptive immune phenotypes in East Palestine residents

Peripheral blood composition was first broadly characterized with complete blood counts (CBC). Red blood cell (RBC) counts,

hematocrit (HCT) levels, mean corpuscular hemoglobin concentrations (MCHC), and overall hemoglobin (HBG) concentrations were significantly higher in EP samples compared to controls (Supplementary Fig. 1A). Additionally, significantly elevated platelet (PLT) concentration and mean platelet volume (MPV) were detected in EP subjects (Supplementary Fig. 1A). Lymphocyte percentage was lower in EP residents, while granulocyte percentage was higher (Supplementary Fig. 1A).

Since CBC data is limited to cell size, shape, and granularity properties, we next used flow cytometry on PBMC samples to obtain a deeper insight into cell-specific alterations within the white blood cell compartment. We initially classified subsets through manual gating (Supplementary Fig. 1B). In line with the reduced lymphocyte concentrations noted by CBC analysis, frequencies of T cells were significantly lower in EP samples (Fig. 1A). Further partitioning into T cell subsets revealed a reduction of CD4+ cells accompanied by an expansion of cytotoxic CD8+ cells in the EP cohort (Fig. 1A). Moreover, EP samples had reduced percentages of naive CD4+ and CD8+ T cells with an expansion of effector memory subsets (Fig. 1A). The EP samples additionally had a lower percentage of B cells with a notably lower frequency of naive and higher frequency of MZ-like B cells compared to controls (Fig. 1B). In contrast, the frequency of innate immune cells was significantly higher in EP samples (Fig. 1C). Within the innate cells, the frequency of monocytes was reduced, and the frequency of NK cells was increased (Fig. 1C). An expansion of immunoregulatory non-classical monocytes was observed within the monocyte population in the EP cohort while frequencies of classical and intermediate monocytes were significantly lower than controls (Fig. 1C). The increase in NK cells was driven by a significantly higher prevalence of cytotoxic CD56^{dim} NK cells in the EP group (Fig. 1C).

To further investigate the differences in immune cell frequencies, we performed a robust integration and batch correction followed by unsupervised clustering and dimensionality reduction using FlowSOM (Flow cytometry data analysis using Self-Organizing Maps), a clustering and visualization algorithm for unsupervised analysis of high-dimensional cytometry data [25]. Because it considers all markers simultaneously rather than two at a time and builds self-organizing maps that provide an overview of marker expression across all cells, FlowSOM can reveal cell subsets that might be overlooked as well as identify rare or unexpected populations that traditional sequential manual gating would miss. FlowSOM analysis generated 30 distinct clusters (Supplementary Fig. 1C). Clusters were identified by relative expression of each marker (Table 2 and Supplementary Fig. 1D). Dimensionality reduction with UMAP was overlaid with FlowSOM clustering to generate a two-dimensional visualization (Fig. 2A).

Seven T cell clusters were identified, three CD4+ and four CD8+, which aligned well with the manual gating strategy (Supplementary Fig. 2A). Overlaying of clusters on manual gating revealed distinct separation between CD4+ and CD8+ T cell subsets (Supplementary Fig. 2B). The clustering of CD4+ T cells was driven by expression of costimulatory CD27, which is essential

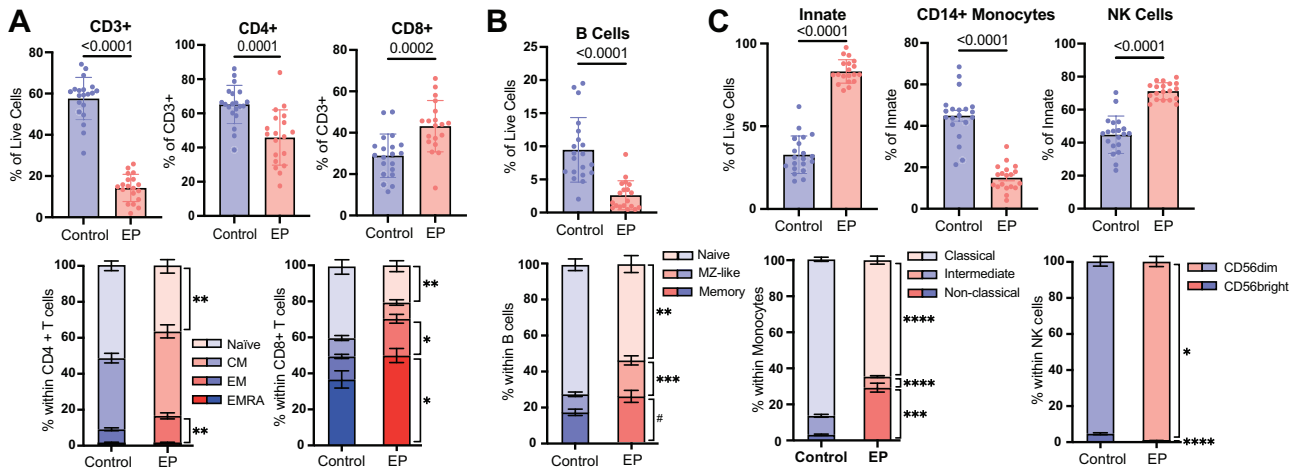


Fig. 1 Flow cytometry reveals altered innate and adaptive immune phenotypes among East Palestine residents. **A** Bar graphs of changes in the frequencies of total T cells (mean, range; control 57.6, 31.1–74.2; EP 14.2, 1.93–25.8), CD4 + T cells (mean, range; control 65.17, 38.6–86.1; EP 45.9, 17.5–83.9), CD8 + T cells (mean, range; control 28.9, 11.5–50.0; EP 43.2, 13.3–66.2) and stacked bar graphs of memory subsets derived from manual gating of flow cytometry phenotyping. Error bars represent the standard error of the mean (SEM). **B** Bar graphs of changes in the frequencies of B cells (mean, range; control 9.5, 2.04–19.5; EP 2.6, 0.46–8.78) and stacked bar graphs of memory subsets derived from manual gating of flow cytometry phenotyping. Error bars represent SEM. **C** Bar graphs of changes in the frequencies of innate cells (mean, range; control 44.9, 21.3–68.5; EP 15.0, 4.02–30.0), monocytes (mean, range; control 44.8, 23.2–70.4; EP 71.2, 63.1–79.6) and stacked bar graphs of subsets derived from manual gating of flow cytometry phenotyping. Error bars represent SEM. (# = $p < 0.1$, * = $p < 0.05$, ** = $p < 0.01$, *** = $p < 0.001$, **** = $p < 0.0001$).

for the differentiation of T memory cells [27]. This marker is expressed on all naïve and most memory T cells but is lost in effector subsets [28]. Within CD4 + T cells, three populations differentiated by CD27^{high}, CD27⁺, and CD27⁻ expression were identified as clusters 1, 2, and 11 respectively (Supplementary Fig. 2B). The CD8 + T cells were clustered based on CD197 and CD45RA marker expression resulting in cluster 18 and 19 containing predominantly CD8 + terminally differentiated effector memory (TEMRA), cluster 20 containing predominantly naïve CD8 +, and cluster 26 containing predominantly effector memory (EM) and central memory (CM) (Supplementary Fig. 2B). T cell cluster distribution across UMAPs indicated noticeable differences between EP and Control cohorts (Fig. 2B, C). Aligning with our manual gating observations, EP samples had a lower percentage of total T cells, a lower percentage of helper CD4 + T cells, and a higher percentage of cytotoxic CD8 + T cells (Fig. 2C). Within the CD4 + subset, the EP cohort had a significantly lower percentage of likely naïve CD27^{high} cluster 1 and a higher percentage of memory CD27⁺ cluster 2 (Fig. 2C). Within the CD8 + subset, a higher proportion of cluster 18 TEMRA and a lower proportion of cluster 20 naïve was expressed in EP samples (Fig. 2C). Only one B cell cluster (#28) was identified. We were therefore unable to distinguish the naïve and memory B cell subsets through FlowSOM analysis (Fig. 2D). However, in line with the decrease of B lymphocytes observed through manual gating, EP samples had significantly lower B cell cluster 28 percentages compared to controls (Fig. 2D).

Within innate cells, we identified four monocyte clusters all expressing CD14 (Supplementary Fig. 3A); clusters 25, 29, and 30 were designated as classical based due to lack of CD16 expression, while cluster 27 was designated as non-classical/intermediate monocytes based on the CD14^{dim} CD16⁺ phenotype (Supplementary Fig. 3B). We combined the frequencies of all monocytes identified clusters and compared their relative percentage among all innate clusters which revealed the percentage of monocytes was significantly lower in the EP cohort, which aligned with the manual gating results (Fig. 3B). An expansion of classical monocyte clusters 25 and 29 was noted for the EP samples (Fig. 3A, B). Six clusters of NK cells were identified based on CD16 and CD56 expression with clusters 12, 21, 22, and 23 being CD16 +

CD56^{dim}, cluster 13 being CD16 + CD56⁻, and cluster 17 being CD16⁻ CD56^{bright} (Fig. 3C). Overall frequency of NK cells was higher in the EP group (Fig. 3D). The percentages of cluster 12 CD16 + CD56^{dim} and cluster 13 CD16 + CD56⁻ NK cells were increased in the EP group (Fig. 3C).

Changes in the inflammatory profiles of East Palestine residents

We next evaluated circulating immune factors via Luminex to observe potential impacts of the derailment exposure on systemic inflammatory markers. Among EP participants, concentrations of the chemoattractants eotaxin, IL-8, MCP-1, MIP-1 β , and CXCL9 were significantly decreased (Fig. 4A). Levels of M-CSF and IL-6, which promote monocyte and macrophage activation, were also decreased in the EP cohort (Fig. 4A). On the other hand, levels of cytokines and growth factors associated with hematopoietic differentiation (IL-3) and tissue repair (IL-4, PDGF-AB/BB, VEGF) were increased in EP samples (Fig. 4A). This was accompanied by elevated levels of proinflammatory cytokines IFN γ , IL-12p40, IL-18, and TNF α (Fig. 4A). The sPLS-DA of analyte concentrations revealed that difference between EP and control immune mediator concentrations was driven predominantly along variate 1 (x-axis) (Fig. 4B). The cytokines which contributed to this separation included PDGF-AB/BB, IL-3, and VEGF which were more highly expressed in the EP cohort and IL-8 and eotaxin which were more highly expressed in the controls (Fig. 4C).

We also investigated functional alteration in the immune cells by exposing PBMC to a cocktail of bacterial TCR agonists to mimic infection and assessing cytokine production using flow cytometry. IL-6 production by classical monocytes, non-classical monocytes, plasmacytoid dendritic cells (pDC), and myeloid dendritic cells (mDC) was diminished (Fig. 4D, E) while that of TNF α was heightened within classical monocytes, pDCs, and mDCs in the EP samples (Fig. 4D, E). Additionally, reduced IL-1 β and enhanced MIP-1 β production were observed within EP classical monocytes (Fig. 4D, E).

DISCUSSION

The East Palestine train derailment resulted in the potential exposure of residents to a variety of chemical compounds

Table 2. Cluster Identification.

Cluster	Markers	Identification
1	CD3 + CD4+ CD27high	T cells; CD4+ CD27high
2	CD3 + CD4 + CD27+	T cells; CD4 + CD27+
3	MEM Score 1	Unidentified
4	MEM Score 1	Unidentified
5	MEM Score 1	Unidentified
6	MEM Score 1	Unidentified
7	MEM Score 1	Unidentified
8	CD16+	Misc. innate
9	CD16+	Misc. innate
10	MEM Score 1	Unidentified
11	CD3 + CD4 + CD27-	T cells; CD4 + CD27-
12	HLA-DR- CD16+ CD56dim (CD45RA-)	NK cells; CD16+ CD56dim (CD45RA-)
13	HLA-DR- CD16 + CD56-	NK cells; CD16 + CD56-
14	CD16+	Misc. Innate
15	CD45RA+	Misc. Innate
16	CD3 + CD4- CD8-	T cells; CD4- CD8-
17	HLA-DR- CD16- CD56bright	NK cells; CD16- CD56bright
18	CD3 + CD8+ CD45RA _{low} CD197-	T cells; CD8 + EM
19	CD3 + CD8 + CD45RA + CD197-	T cells; CD8 + TEMRA
20	CD3 + CD8 + CD45 + CD197+	T cells; CD8+ naïve
21	HLA-DR- CD16+ CD56dim	NK cells; CD16+ CD56dim
22	HLA-DR- CD16+ CD56dim	NK cells; CD16+ CD56dim
23	HLA-DR- CD16+ CD56dim	NK cells; CD16+ CD56dim
24	HLA-DR + CD123 + CD45RA+	Dendritic cells
25	HLA-DR + CD14 + CD16-	Monocytes; Classical
26	CD3 + CD8 + CD45- CD197 _{low}	T cells; CD8 + CM & EM
27	HLA-DR+ CD14 _{low} CD16+	Monocytes; Non-classical & Intermediate
28	CD20 + HLA-DR+	B cells
29	HLA-DR + CD14 + CD16-	Monocytes; Classical
30	HLA-DR + CD14 + CD16-	Monocytes; Classical

Key makers used for the identification of clusters and the identified cluster. Marker expression was scored through marker enrichment modeling (MEM) in reference to all clusters.

associated with detrimental health effects. Environmental pollutant exposure has been linked to immune alterations [22]. VOCs, such as vinyl chloride, have been linked to increased inflammation, altered immune cell development, and altered immune activation [29]. Here, we performed a broad investigation of circulating immune cells from residents of East Palestine compared to age and sex matched control participants from California.

We found increased RBCs and hemoglobin in the EP residents compared to controls. This increase could indicate a compensatory mechanism to enhance oxygen transport. The increased RBCs and MPV observed in EP samples align with trends observed following organic solvent exposure among car painters and mechanics [30]. Air monitoring performed between the 20th and 21st of February 2023 revealed high levels of acrolein and the identification of unique compounds at concentrations above background levels [13]. Acrolein is a known respiratory [31] and ocular irritant [32] with potential immunological effects. Rodent studies have shown decreased bactericidal activity, decreased frequency of alveolar macrophages, and suppressed pulmonary inflammation following acrolein exposure [33]. The difference in cytokine profile between EP and controls was predominantly driven by growth factors with increased levels of VEGF and

PDGF. Platelets release both VEGF and PDGR, which are involved in the expansion of erythropoiesis [34–36], indicating an involvement of VEGF and PDGR in the increased RBCs and MPV EP counts. These growth factors are suggestive of increased wound healing and blood vessel repair, potentially due to damage caused by irritant exposure. Long-term inhalation exposure to VOCs is associated with a proinflammatory response driven by the production of reactive oxygen species (ROS) [29]. These ROS activate transcription factors and result in the production of proinflammatory mediators, driving oxidative stress and tissue damage at the site of inflammation [29]. Excessive damage caused by VOC-induced oxidative stress would likely induce an upregulation of growth factors, such as VEGF and PDGR, to promote tissue repair.

Our data showed overall T- and B-lymphocyte frequencies within the expected range in the control group (CD3+ ~50–70% of total PBMCs, CD4+ ~50–70% of CD3+ cells, CD8+ ~25–35% of CD3+ cells, and B cells ~10–15% of total PBMCs) [37, 38]. In contrast, decreased T-lymphocyte percentages, particularly naïve, were observed in the EP cohort, suggesting a perturbation in East Palestine participants. In addition to lower lymphocyte frequencies, a shift from naïve to memory subsets was noted in both T and B cells. Naïve T and B cells differentiate after specific antigen

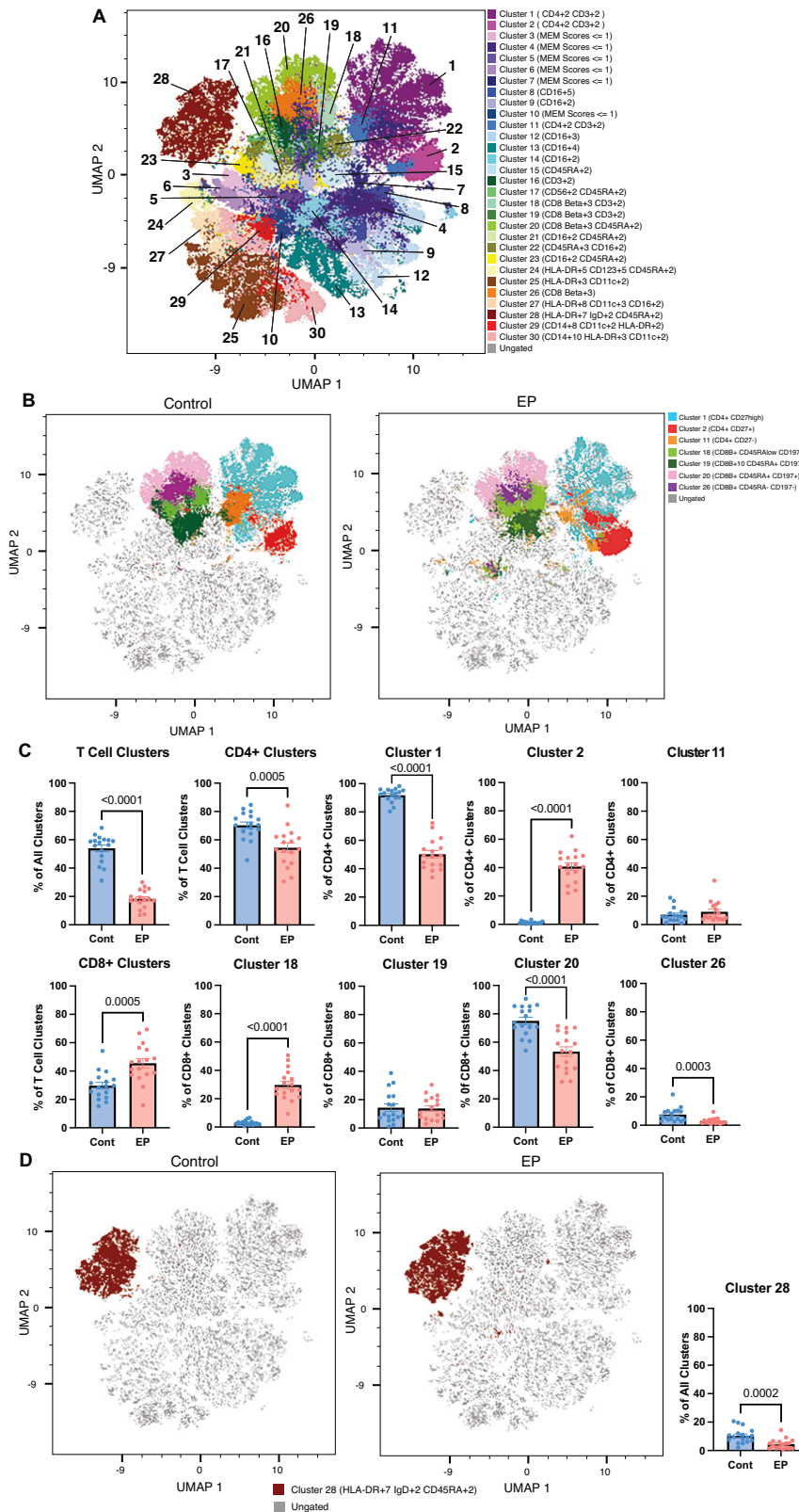


Fig. 2 Enhanced T cell maturation, increased percentage of cytotoxic CD8 + T cells, and decreased B cells in East Palestine residents. **A** UMAP dimensionality reduction colored according to the 30 clusters identified with FlowSOM. Marker enrichment modeling (MEM) scoring employed to provide quantitative marker comparisons between clusters for identification. **B** UMAPs of the Control and EP cohorts colored according to their T cell cluster distribution. **C** Bar plots comparing cluster percentages between Control and EP. **D** UMAPs of the Control and EP cohorts colored according to their B cell cluster distribution. Bar plot comparing B cell cluster percentages between Control and EP.

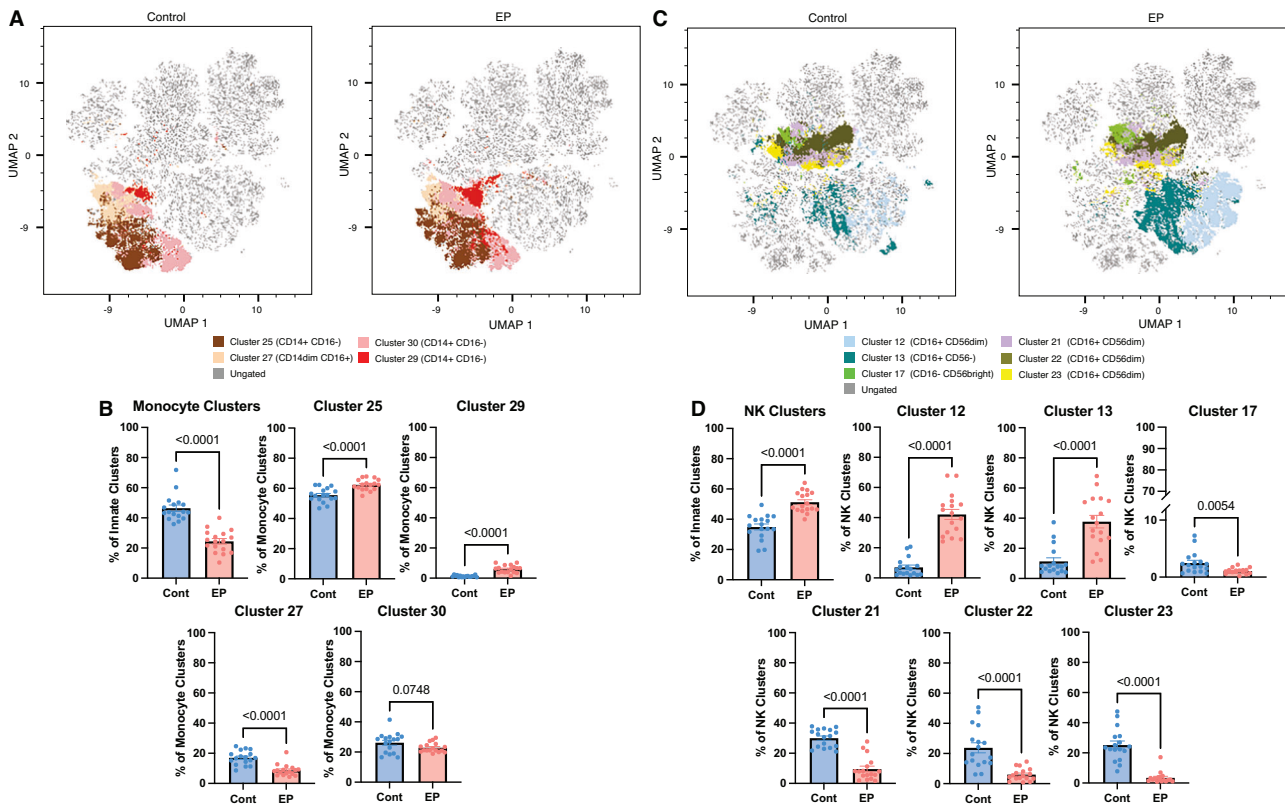


Fig. 3 Altered innate immune phenotype in East Palestine residents. **A** UMAPs of the Control and EP cohorts colored according to their monocyte cluster distribution. **B** Bar plots comparing monocyte cluster percentages between Control and EP. **C** UMAPs of the Control and EP cohorts colored according to their NK cluster distribution. **D** Bar plots comparing NK cluster percentages between Control and EP.

exposure to generate long-lived memory cells to respond upon re-exposure [39]. Decreased naïve CD8+ T cells are associated with increased susceptibility to infections and immunodeficiency with aging [40]. ROS are known to contribute to the activation and proliferation of T cells, with studies indicating VOC exposure notably alters T cell phenotypes and proportions [29, 41]. VOCs have been implicated in the skewing of T cell polarization toward Th2, resulting in increased IgE production and contributing to heightened allergic response [42, 43]. The ROS induced by VOCs elicits the production of autoreactive T cells, and exposure is associated with increased risk of developing autoimmune disorders, such as rheumatoid arthritis, multiple sclerosis, and ulcerative colitis [29, 44]. Certain VOCs have specific impacts on T cell percentages within the peripheral blood. For example, trichloroethylene exposure is associated with decreased numbers of CD4+ naïve, CD4+ EM, and CD8+ naïve cells [45, 46]. Overall, increased percentages of mature lymphocytes indicate heightened immune activation, potentially indicating a state of chronic or prolonged inflammation within the EP cohort.

While lymphocyte frequencies decreased in EP residents compared to controls, granulocytes conversely increased. Due to the vent and burn of five cars of vinyl chloride, another chemical class of concern is dioxins, a group of persistent organic pollutants formed during the combustion of polyvinylchloride (PVC) [47, 48]. Dioxins can alter human hematopoietic stem cell differentiation toward myeloid lineages, impairing lymphopoiesis and suppressing T and B lymphocyte development [49]. The alteration in hematopoiesis we observed additionally links to the increase in IL-3 plasma concentrations among EP samples. IL-3 is a stimulator of hematopoietic stem cell differentiation and is associated with emergency hematopoiesis initiated during sepsis and parasitic infections [50–52]. The increase in IL-3 concentrations potentially indicates a state of acute inflammation as myeloid cells are

generated for irritant clearance. Despite reduced lymphopoiesis being observed and the potential for enhanced myelopoiesis due to increased IL-3, percentages of monocytes remained lower in EP samples compared to controls. This aligns with prior studies indicating dioxins interact with the aryl hydrocarbon receptor (AhR), which is highly expressed on monocytes [53–55]. It has been shown that AhR ligands interfere with myeloid progenitor cell commitment to monocyte and dendritic cell lineages while granulopoiesis remains unaffected [56]. Alternatively, the reduction of monocytes could be driven by migration from the peripheral blood to the site of inflammation. Acrolein specifically has been associated with macrophage chemotaxis and migration, particularly in the context of inhalation via tobacco smoke [57].

Interestingly, our controls exhibited elevated eotaxin concentrations comparable to levels reported in individuals with allergic rhinitis or asthmatic inflammation [58, 59]. Given that these participants reported no occurrence of allergy or asthma, this elevation may be attributable to environmental exposures specific to this geographic region, which experienced a prolonged drought between 2012 and 2015 and widespread wildfires during the collection period. Inhalation of wildfire-associated particulate matter has been observed to elevate eotaxin concentrations. Although our controls reflect typical immune population percentages that occur in the general population, geographic influences should be considered.

Importantly, the psychological stress commonly induced following disasters has repeatedly been linked to immune dysregulation and noted to alter immune responsiveness and cytokine production [60–62]. Indeed, during the month following the derailment, health surveys of East Palestine reported anxiety as one of the most experienced symptoms [11]. The proinflammatory cytokines IL-6 and TNF- α are noted as primary markers of stress-related inflammation, with concentrations increasing with

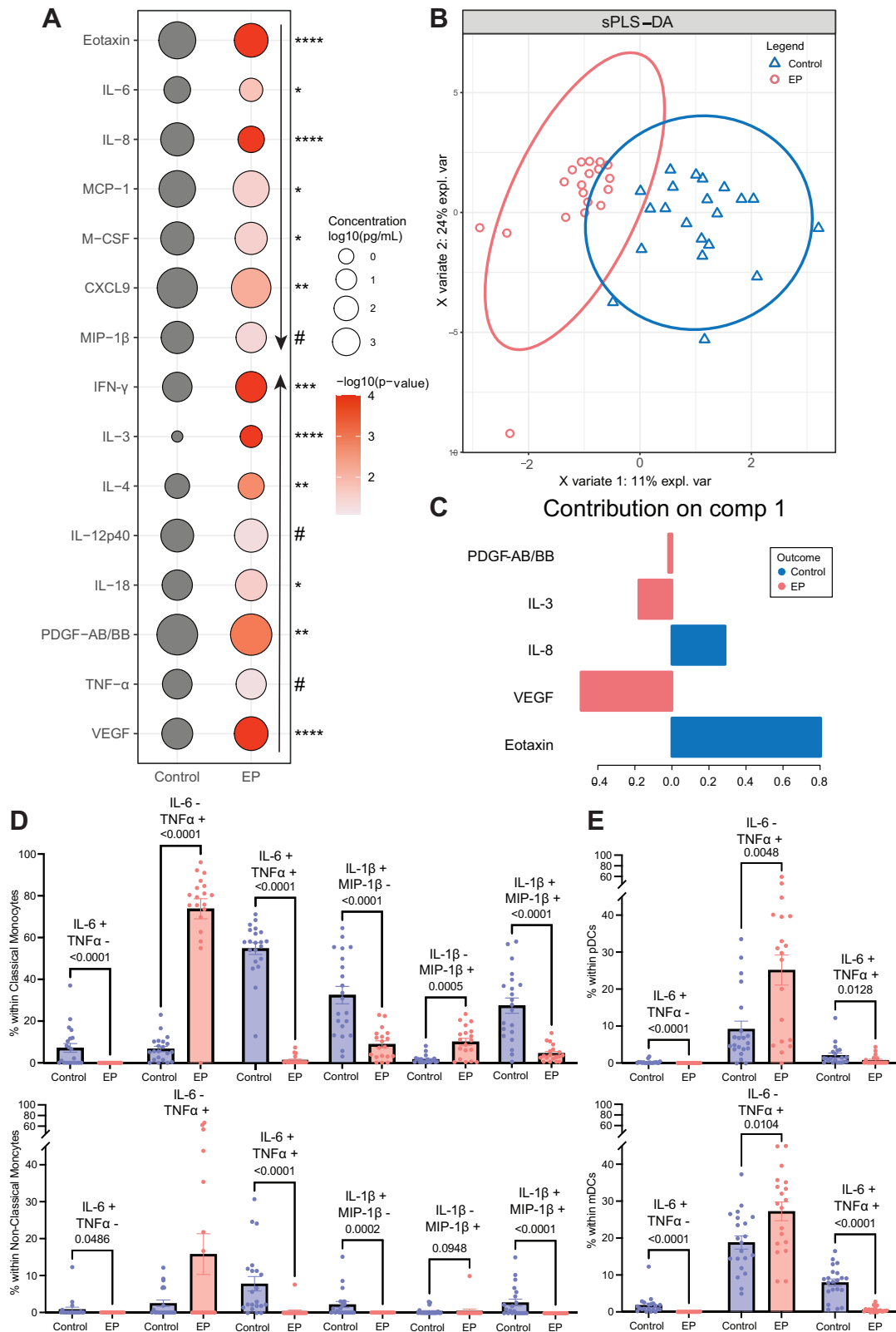


Fig. 4 Altered inflammatory profile in East Palestine residents. **A** Bubble plot comparing plasma immune mediators between EP and control. Size represents analyte concentration, and color represents the calculated p -value between the two groups. (# = $p < 0.1$, * = $p < 0.05$, ** = $p < 0.01$, *** = $p < 0.001$, **** = $p < 0.0001$). **B** Sparse partial least squares discriminant analysis (sPLS-DA) on plasma immune mediator concentrations. The X- and Y-axis refer to the first and second components, respectively. The percentage of variance for each component is in parentheses on the associated axis. **C** The contribution of the immune mediators to the first component. **D** Frequencies of IL-6/TNF α and IL-1 β / MIP-1 β secretions by classical monocytes and non-classical monocytes following bacterial stimulation. **E** Frequencies of IL-6 / TNF α and IL-1 β / MIP-1 β secretions by pDCs and mDCs following bacterial stimulation.

depression, anxiety, and post-traumatic stress disorder [60–64]. While we observed heightened TNF- α plasma levels and responsiveness to bacterial stimulation in East Palestine samples, IL-6 was notably diminished.

In summary, this study provides the first immunotoxicological insights into the impact of exposure to pollutants in East Palestine residents 5 months following the derailment and potential exposure. Although this study provides a foundation for additional investigations into altered immunity among East Palestine residents, it is not without limitations. Our data is limited to 19 exposed participants. Future investigations will increase enrollment and incorporate more residents. Importantly, the sex and age-matched controls used here were from southern California, which is geographically and environmentally varied from East Palestine, Ohio. Geographical factors and location contribute to altered immune landscapes and phenotypes. Socioeconomic differences between the two regions are another important consideration. U.S. Census American Community Survey (ACS) data indicates that in 2016, Riverside, CA had a higher median income and a higher percentage of adults holding a bachelor's degree compared to East Palestine, OH in 2023 [65]. However, Riverside, CA, had a higher median housing cost and estimated poverty percentage of $16.5 \pm 0.4\%$ compared to East Palestine, OH, in 2023 at $9.5 \pm 3.6\%$ [65]. The largest socioeconomic differences between these two cohorts are derived from differences in educational attainment and economic diversity that come with a larger, more urban setting. Retrospective studies with geographically and socioeconomically matched unexposed controls will be critical.

While both Control and EP samples were collected and processed with the same methods and then cryopreserved under the same conditions, it is important to consider the impact of long-term storage on cell percentages and responsiveness. Long-term cryopreservation is known to decrease cell viability; however, studies have shown that PBMC viability remains relatively high even after long-term storage, with a median viability of approximately 80% after 11 years [66]. Prior studies comparing fresh and cryopreserved PBMCs have reported minimal differences in immune phenotypes across major cell subsets [67, 68]. Nevertheless, it is important to consider the bias introduced by different durations of cryopreservation on cell proportions and responsiveness. Future work should incorporate controls collected, processed, and stored at the same time.

DATA AVAILABILITY

The data supporting the findings of this study are available in the Mendeley Data repository at <https://doi.org/10.17632/wc95cnc3z5.1>.

REFERENCES

- United States Environmental Protection Agency (EPA). East Palestine, Ohio Train Derailment Background. Available from: <https://www.epa.gov/east-palestine-oh-train-derailment/background>.
- Agency for Toxic Substances and Disease Registry (ATSDR). Medical Management Guideline for Vinyl Chloride. Atlanta, GA: U.S. Department of Health and Human Services, CDC [updated 2014 October 21; cited 2025 December 10]. Available from: <https://www.cdc.gov/TSP/MMG/MMGDetails.aspx?mmgid=278&toxid=51>.
- National Institute for Occupational Safety and Health (NIOSH). Butyl acrylate, Atlanta, GA: U.S. Department of Health and Human Services, CDC. Available from: <https://www.cdc.gov/niosh/npg/npgd0075.html>.
- National Center for Biotechnology Information. PubChem Compound Summary for CID 7636, 2-Ethylhexyl acrylate. Available from: <https://pubchem.ncbi.nlm.nih.gov/compound/2-Ethylhexyl-acrylate>.
- National Center for Biotechnology Information. PubChem Compound Summary for CID 8255, Isobutylene. Available from: <https://pubchem.ncbi.nlm.nih.gov/compound/Isobutylene>.
- National Center for Biotechnology Information. PubChem Compound Summary for CID 8133, 2-Butoxyethanol. Available from: <https://pubchem.ncbi.nlm.nih.gov/compound/2-Butoxyethanol>.
- Centers for Disease Control and Prevention. Chemical Emergencies Benzene Chemical Fact Sheet Atlanta, GA: U.S. Department of Health and Human Services, CDC. Available from: <https://www.cdc.gov/chemical-emergencies/chemical-fact-sheets/benzene.html>.
- Ohio Emergency Management Agency (EMA). East Palestine Urgent Evacuation Notice: Columbus, OH: Emergency Management Agency. Available from: <https://ema.ohio.gov/media-publications/news/dewine-020523>.
- Ohio Emergency Management Agency (EMA). East Palestine Update: Evacuation Area Extended, Controlled Release of Rail Car Contents Planned for 3:30 p.m. Columbus, OH: Emergency Management Agency. Available from: <https://ema.ohio.gov/media-publications/news/dewine-020623>.
- Governor of Ohio. East Palestine Update: Residents Can Safely Return Home. Available from: <https://governor.ohio.gov/media/news-and-media/east-palestine-update-residents-can-safely-return-home-02082023>.
- Ohio Emergency Management Agency (EMA). East Palestine Update - 3/3/23 Columbus, OH: Emergency Management Agency. Available from: <https://ema.ohio.gov/media-publications/news/030323-east-palestine-update>.
- National Academies of Sciences, Engineering, and Medicine; Health and Medicine Division; Board on Health Sciences Policy. Public Health Research and Surveillance Priorities from the East Palestine Train Derailment: In Proceedings of a Workshop—in Brief. Wollek S, Masiello M, Snair J, editors. Washington: National Academies Press; 2024.
- Oladeji O, Saitas M, Mustapha T, Johnson NM, Chiu WA, Rusyn I, et al. Air Pollutant patterns and human health risk following the east palestine, ohio, train derailment. *Environ Sci Technol Lett*. 2023;10:680–5.
- Strum M, Scheffe R. National review of ambient air toxics observations. *J Air Waste Manag Assoc*. 2016;66:120–33.
- Bashir H, Mahalwar G, Henry T. The East Palestine disaster: the potential toxic effects of vinyl chloride exposure on cardiovascular health. *Cureus*. 2023;15:e46835.
- Nogueira LM, Sherman JD, Shultz JM. Derailing carcinogens: oncologists and the Ohio train derailment. *JAMA Oncol*. 2024;10:25–6.
- Sergi CM. Pediatric hepatic angiosarcoma (PHAS) and vinyl chloride—a ghost of the past may loom over East Palestine, OH, and beyond: a critical commentary. *Diagnostics*. 2023;13.
- Sun W. The devastating health consequences of the Ohio derailment: a closer look at the effects of vinyl chloride spill. *Int J Environ Res Public Health*. 2023;20.
- Babich R, Sneeringer K, Gandhi K, Miller J, Nair A, Watkins S, et al. Pennsylvania first responder assessment of chemical exposure survey following the East Palestine, Ohio. *Disaster Med Public Health Prep*. 2025;19:e149.
- Chen L, Deng H, Cui H, Fang J, Zuo Z, Deng J, et al. Inflammatory responses and inflammation-associated diseases in organs. *Oncotarget*. 2018;9:7204–18.
- Kreitinger JM, Beamer CA, Shepherd DM. Environmental immunology: lessons learned from exposure to a select panel of immunotoxicants. *J Immunol*. 2016;196:3217–25.
- Luster MI. A historical perspective of immunotoxicology. *J Immunotoxicol*. 2014;11:197–202.
- Lewis SA, Sureshchandra S, Zulu MZ, Doratt B, Jankeel A, Ibraim IC, et al. Differential dynamics of peripheral immune responses to acute SARS-CoV-2 infection in older adults. *Nat Aging*. 2021;1:1038–52.
- Doratt BM, Sureshchandra S, True H, Rincon M, Marshall NE, Messaoudi I. Mild/asymptomatic COVID-19 in unvaccinated pregnant mothers impairs neonatal immune responses. *JCI Insight*. 2023;8:e172658.
- Van Gassen S, Callebaut B, Van Helden MJ, Lambrecht BN, Demeester P, Dhaene T, et al. FlowSOM: using self-organizing maps for visualization and interpretation of cytometry data. *Cytom A*. 2015;87:636–45.
- Rohart F, Gautier B, Singh A, Le Cao KA. mixOmics: an R package for 'omics feature selection and multiple data integration. *PLoS Comput Biol*. 2017;13:e1005752.
- Hendriks J, Gravestain LA, Tesselaar K, van Lier RA, Schumacher TN, Borst J. CD27 is required for generation and long-term maintenance of T cell immunity. *Nat Immunol*. 2000;1:433–40.
- Schiott A, Lindstedt M, Johansson-Lindbom B, Roggen E, Borrebaeck CA. CD27-CD4+ memory T cells define a differentiated memory population at both the functional and transcriptional levels. *Immunology*. 2004;113:363–70.
- Ogbodo JO, Arazu AV, Iguh TC, Onwodi NJ, Ezike TC. Volatile organic compounds: a proinflammatory activator in autoimmune diseases. *Front Immunol*. 2022;13:928379.
- Beving H, Tornling G, Olsson P. Increased erythrocyte volume in car repair painters and car mechanics. *Br J Ind Med*. 1991;48:499–501.
- Matsumoto M, Yamano S, Senoh H, Umeda Y, Hirai S, Saito A, et al. Carcinogenicity and chronic toxicity of acrolein in rats and mice by a two-year inhalation study. *Regul Toxicol Pharmacol*. 2021;121:104863.
- Weber-Tschopp A, Fischer T, Gierer R, Grandjean E. [Experimentally induced irritating effects of acrolein on men (author's transl)]. *Int Arch Occup Environ Health*. 1977;40:117–30.

33. Kim BG, Lee PH, Lee SH, Hong J, Jang AS. Claudins, VEGF, Nrf2, Keap1, and nonspecific airway hyper-reactivity are increased in mice co-exposed to allergen and acrolein. *Chem Res Toxicol*. 2019;32:139–45.
34. Greenwald AC, Licht T, Kumar S, Oladipupo SS, Iyer S, Grunewald M, et al. VEGF expands erythropoiesis via hypoxia-independent induction of erythropoietin in noncanonical perivascular stromal cells. *J Exp Med*. 2019;216:215–30.
35. Ye JY, Chan GC, Qiao L, Lian Q, Meng FY, Luo XQ, et al. Platelet-derived growth factor enhances platelet recovery in a murine model of radiation-induced thrombocytopenia and reduces apoptosis in megakaryocytes via its receptors and the PI3-k/Akt pathway. *Haematologica*. 2010;95:1745–53.
36. Zymek P, Bujak M, Chatila K, Cieslak A, Thakker G, Entman ML, et al. The role of platelet-derived growth factor signaling in healing myocardial infarcts. *J Am Coll Cardiol*. 2006;48:2315–23.
37. Yi JS, Rosa-Bray M, Staats J, Zakroscopy P, Chan C, Russo MA, et al. Establishment of normative ranges of the healthy human immune system with comprehensive polychromatic flow cytometry profiling. *PLoS ONE*. 2019;14:e0225512.
38. Chang ST, Chuang YF, Li AH, Fan YT, Liao MR, Chen IY, et al. Age-dependent immune profile in healthy individuals: an original study, systematic review and meta-analysis. *Immun Ageing*. 2024;21:75.
39. Farber DL, Yudanin NA, Restifo NP. Human memory T cells: generation, compartmentalization and homeostasis. *Nat Rev Immunol*. 2014;14:24–35.
40. Fagnoni FF, Vescovini R, Passeri G, Bologna G, Pedrazzoni M, Lavagetto G, et al. Shortage of circulating naive CD8(+) T cells provides new insights into immunodeficiency in aging. *Blood*. 2000;95:2860–8.
41. Morris G, Gevezova M, Sarafian V, Maes M. Redox regulation of the immune response. *Cell Mol Immunol*. 2022;19:1079–101.
42. Bonisch U, Bohme A, Kohajda T, Mogel I, Schutze N, von Bergen M, et al. Volatile organic compounds enhance allergic airway inflammation in an experimental mouse model. *PLoS ONE*. 2012;7:e39817.
43. Lehmann I, Rehwagen M, Diez U, Seiffart A, Rolle-Kampczyk U, Richter M, et al. Enhanced in vivo IgE production and T cell polarization toward the type 2 phenotype in association with indoor exposure to VOC: results of the LARS study. *Int J Hyg Environ Health*. 2001;204:211–21.
44. Lei T, Qian H, Yang J, Hu Y. The exposure to volatile organic chemicals associates positively with rheumatoid arthritis: a cross-sectional study from the NHANES program. *Front Immunol*. 2023;14:1098683.
45. Hosgood HD 3rd, Zhang L, Tang X, Vermeulen R, Hao Z, Shen M, et al. Occupational exposure to formaldehyde and alterations in lymphocyte subsets. *Am J Ind Med*. 2013;56:252–7.
46. Hosgood HD 3rd, Zhang L, Tang X, Vermeulen R, Qiu C, Shen M, et al. Decreased numbers of CD4(+) naive and effector memory T cells, and CD8(+) naive T cells, are associated with trichloroethylene exposure. *Front Oncol*. 2011;1:53.
47. Haynes EN, Eskenazi B, Hilbert TJ, Brancato C, Holland N, Kim C, et al. Serum dioxin levels in a subset of participants of the east palestine, ohio train derailment health tracking study. *Environ Sci Technol Lett*. 2024;11:673–8.
48. Zhang M, Buekens A, Jiang X, Li X. Dioxins and polyvinylchloride in combustion and fires. *Waste Manag Res*. 2015;33:630–43.
49. Khan D, Crawford RB, Kaminski NE. Regulation of in vitro human hematopoietic differentiation by dioxin-like compounds. *Toxicology*. 2025;514:154136.
50. Lantz CS, Boesiger J, Song CH, Mach N, Kobayashi T, Mulligan RC, et al. Role for interleukin-3 in mast-cell and basophil development and in immunity to parasites. *Nature*. 1998;392:90–3.
51. Podolska MJ, Grutzmann R, Pilarsky C, Benard A. IL-3: key orchestrator of inflammation. *Front Immunol*. 2024;15:1411047.
52. Weber GF, Chousterman BG, He S, Fenn AM, Nairz M, Anzai A, et al. Interleukin-3 amplifies acute inflammation and is a potential therapeutic target in sepsis. *Science*. 2015;347:1260–5.
53. Komura K, Hayashi S, Makino I, Poellinger L, Tanaka H. Aryl hydrocarbon receptor/dioxin receptor in human monocytes and macrophages. *Mol Cell Biochem*. 2001;226:107–18.
54. Tian J, Feng Y, Fu H, Xie HQ, Jiang JX, Zhao B. The aryl hydrocarbon receptor: a key bridging molecule of external and internal chemical signals. *Environ Sci Technol*. 2015;49:9518–31. <https://doi.org/10.1021/acs.est.5b00385>.
55. de Juan A, Tabtim-On D, Coillard A, Becher B, Goudot C, Segura E. The aryl hydrocarbon receptor shapes monocyte transcriptional responses to interleukin-4 by prolonging STAT6 binding to promoters. *Sci Signal*. 2024;17:eadn6324.
56. Platzner B, Richter S, Kneidinger D, Waltenberger D, Woisetschlager M, Strobl H. Aryl hydrocarbon receptor activation inhibits in vitro differentiation of human monocytes and Langerhans dendritic cells. *J Immunol*. 2009;183:66–74.
57. DeJarnett N, Conklin DJ, Riggs DW, Myers JA, O'Toole TE, Hamzeh I, et al. Acrolein exposure is associated with increased cardiovascular disease risk. *J Am Heart Assoc*. 2014;3.
58. Lilly CM, Woodruff PG, Camargo CA Jr, Nakamura H, Drazen JM, Nadel ES, et al. Elevated plasma eotaxin levels in patients with acute asthma. *J Allergy Clin Immunol*. 1999;104:786–90.
59. Jahnz-Róyk K, Plusa T, Mierzejewska J. Eotaxin in serum of patients with asthma or chronic obstructive pulmonary disease: relationship with eosinophil cationic protein and lung function. *Mediators Inflamm*. 2000;9:175–9.
60. Glaser R, Kiecolt-Glaser JK. Stress-induced immune dysfunction: implications for health. *Nat Rev Immunol*. 2005;5:243–51.
61. Fagundes CP, Glaser R, Kiecolt-Glaser JK. Stressful early life experiences and immune dysregulation across the lifespan. *Brain Behav Immun*. 2013;27:8–12.
62. Michopoulos V, Powers A, Gillespie CF, Ressler KJ, Jovanovic T. Inflammation in fear- and anxiety-based disorders: PTSD, GAD, and beyond. *Neuropsychopharmacology*. 2017;42:254–70.
63. Penninx BW, Kritechevsky SB, Yaffe K, Newman AB, Simonsick EM, Rubin S, et al. Inflammatory markers and depressed mood in older persons: results from the Health, Aging and Body Composition study. *Biol Psychiatry*. 2003;54:566–72.
64. Glaser R, Robles TF, Sheridan J, Malarkey WB, Kiecolt-Glaser JK. Mild depressive symptoms are associated with amplified and prolonged inflammatory responses after influenza virus vaccination in older adults. *Arch Gen Psychiatry*. 2003;60:1009–14.
65. U.S. Census Bureau. American Community Survey, ACS 5-Year Estimates: Subject Tables. Available from: <https://data.census.gov/table>.
66. Sun J, Gao M, Li K, Qin L, Sun H, Qiao G, et al. Quality of cryopreserved peripheral blood mononuclear cells recovered from the hepatitis/AIDS biobank. *Biopreserv Biobank*. 2018;16:397–401.
67. Tompa A, Johansson J, Islander U, Faresjö M. Flow cytometric immunophenotyping: minimal differences in fresh and cryopreserved peripheral blood mononuclear cells versus whole blood. *Biomedicines*. 2024;12:2319.
68. Verschoor CP, Kohli V, Balion C. A comprehensive assessment of immunophenotyping performed in cryopreserved peripheral whole blood. *Cytom B Clin Cytom*. 2018;94:662–70.

ACKNOWLEDGEMENTS

We recognize the role of team science and wish to acknowledge the effort of the following for their contribution to this study: Jody Alden, RN, Delores Silverthorn, RN, Danielle McBride, PhD, Pastor Fritz Nelson, Geraldine Moore, and the First United Presbyterian church of East Palestine Congregation, and the East Palestine Health Tracking Study, Community Advisory Board, chaired by Misti Allison, MPH. This work was supported by the UK Flow Cytometry & Immune Monitoring core facility (RRIDSCR_026358).

AUTHOR CONTRIBUTIONS

SBW performed experiments, analyzed data, generated visualizations, wrote the original draft of the manuscript, and contributed to review and editing. HH performed experiments, analyzed data, and contributed to visualization. SG contributed to conceptualization, methodology, and manuscript review. TJH contributed to data curation, project administration, and manuscript review and editing. CB contributed to data curation and project administration. ENH contributed to conceptualization, methodology, funding acquisition, and manuscript review and editing. IM contributed to conceptualization, methodology, resources, supervision, and manuscript review and editing.

FUNDING

This study was supported in part by NIH/NIEHS P30ES026529; R21ES036036; OT2ES038696 and NIH/NCATS UL1TR001998. Its contents are solely the responsibility of the authors and do not necessarily represent the official views of the NIH/NIEHS.

COMPETING INTERESTS

The authors declare no competing interests.

ADDITIONAL INFORMATION

Supplementary information The online version contains supplementary material available at <https://doi.org/10.1038/s41370-026-00918-y>.

Correspondence and requests for materials should be addressed to Erin N. Haynes or Ilhem Messaoudi.

Reprints and permission information is available at <http://www.nature.com/reprints>

Publisher's note Springer Nature remains neutral with regard to jurisdictional claims in published maps and institutional affiliations.



Open Access This article is licensed under a Creative Commons Attribution-NonCommercial-NoDerivatives 4.0 International License, which permits any non-commercial use, sharing, distribution and reproduction in any medium or format, as long as you give appropriate credit to the original author(s) and the source, provide a link to the Creative Commons licence, and indicate if you modified the licensed material. You do not have permission under this licence to share adapted material derived from this article or parts of it. The images or other third party material in this article are included in the article's Creative Commons licence, unless indicated otherwise in a credit line to the material. If material is not included in the article's Creative Commons licence and your intended use is not permitted by statutory regulation or exceeds the permitted use, you will need to obtain permission directly from the copyright holder. To view a copy of this licence, visit <http://creativecommons.org/licenses/by-nc-nd/4.0/>.

© The Author(s) 2026